Atmosphere **2012**, *3*, 537-556; doi:10.3390/atmos3040537

OPEN ACCESS

atmosphere

ISSN 2073-4433

www.mdpi.com/journal/atmosphere

Article

Modelling Regional Surface Energy Exchange and Boundary Layer Development in Boreal Sweden — Comparison of Mesoscale Model (RAMS) Simulations with Aircraft and Tower Observations

Elena V. Kvon *, Janno Tuulik, Meelis Mölder and Anders Lindroth

Department of Physical Geography and Ecosystem Science, Lund University, Sölvegatan 12, SE-22362 Lund, Sweden; E-Mails: jannotuulik@gmail.com (J.T.); meelis.molder@nateko.lu.se (M.M.); anders.lindroth@nateko.lu.se (A.L.)

* Authors to whom correspondence shall be addressed; E-Mail: elena.kvon@nateko.lu.se; Tel.: +46-46-222-1725; Fax: +46-46-222-0321.

Received: 7 July 2012; in revised form: 25 September 2012 / Accepted: 15 October 2012 / Published: 30 October 2012

Abstract: Simulation of atmospheric and surface processes with an atmospheric model (RAMS) during a period of ten days in August 2001 over a boreal area in Sweden were compared to tower measurements and aircraft measurements of vertical profiles as well as surface fluxes from low altitude flights. The shape of the vertical profiles was simulated reasonably well by the model although there were significant biases in absolute values. Surface fluxes were less well simulated and the model showed considerable sensitivity to initial soil moisture conditions. The simulations were performed using two different land cover databases, the original one supplied with the RAMS model and the more detailed CORINE database. The two different land cover data bases resulted in relatively large fine scale differences in the simulated values. The conclusion of this study is that RAMS has the potential to be used as a tool to estimate boundary layer conditions and surface fluxes and meteorology over a boreal area but also that further improvement is needed.

Keywords: RAMS; mesoscale climate; boreal region; Norunda tower; airborne data

1. Introduction

Interactions between the land surface and the atmosphere play an important role in the climate system. The climate is modified as a result of the energy exchange at the surface and this means that changes in the land cover, or changes in the functioning of the existing vegetation will have implications for the temperature and moisture content of the atmosphere. Modelling is the obvious tool for analysing the complex interaction between soil, plants and atmosphere. Examples of important feedbacks are soil moisture, which can greatly modify the partitioning between latent and sensible heat, which in turn affects the temperature and moisture of the atmosphere as well as the height of the boundary layer. Land cover and vegetation dynamics are other examples of factors that have important effects on the energy partitioning at the land surface. Today's coupled global and regional climate models do have some of these features (e.g., [1–4]) but the large scale at which they operate makes them less suited to the detailed analysis of some questions, e.g., land-cover patchiness. Eastman [5] discussed this issue and concluded that what is needed is a highly mechanistic model, which operates at a scale where vegetation features at landscape and local scale can be incorporated in a realistic manner.

A mesoscale model with a well-developed land-surface scheme which fulfils the requirements outlined above seems to be a relevant choice and several such models have been developed of which a few are available for non-experts on model development. One of the modelling systems that are used by several groups is RAMS [6]. RAMS generally scores well in model comparisons; Cox [7] compared four mesoscale models: the Regional Atmospheric Modelling System, the Mesoscale Model 5 (MM5), the Navy operational Regional Prediction System Version 6 (NORAPS6) and the Relocatable Windows Model (RWM) and found that both RAMS and MM5 performed better than the other two models. The Texas Natural Resources Conservation Commission [8] performed RAMS and MM5 simulations over the Houston area for the 8–11 September 1993 ozone episode and found that RAMS simulated sea breeze formation better than MM5. Our application concerns the boreal region and as far as we know, RAMS has never been applied to this region although other mesoscale models have (e.g., [9–12]).

Boreal ecosystems play an important role in the Earth system for several reasons: they occupy a large proportion of the terrestrial surface, its structure and functioning are sensitive to subtle changes in climate and many of the possible functional changes might have large effects on the atmosphere [13]. The future climate scenarios also show that the changes will be greatest at high latitudes and there are many sensitive ecosystems, which might be strongly affected by the anticipated changes in climate. In the Nordic region the boreal landscape is characterized by a mosaic of forest stands of different age and density, strongly influenced by management, agricultural fields, lakes and wetlands. The degree of fragmentation varies largely and the scale of the patches is often much less than one km. In order to assess the importance of the differences in land-cover on, e.g., surface fluxes and atmospheric conditions it is important to be able to use a model which has a relatively high spatial resolution; with the nested function of RAMS, such resolution can be obtained.

For practical as well as for scientific applications it is crucial to understand the strengths, weaknesses and limitations of mesoscale models and this can best be done by testing and evaluation against observations which, in the case of RAMS has been done quite extensively (e.g., [14–20]). The RAMS modelling system is most often used as a limited area model, and many of its parameterizations have been designed for mesoscale or high resolution cloud scale grids. In the present work we compare

RAMS v4.4 [21] results with airborne and tower observations that were undertaken during August 2001 in a region in central Sweden consisting of a typical boreal landscape with quite a patchy structure. This area was studied previously during the NOPEX experiment [22–25]. The aim of this study is to assess the capability of the RAMS modelling system to simulate surface fluxes and atmospheric conditions in a boreal setting and also to assess the sensitivity to land-cover representation and different initial conditions.

2. Materials and Methods

2.1. Area

The 78 km × 78 km area subject to detailed investigation is located in the southern part of the boreal zone in central Sweden. The area is characterized by an irregular mixture of forest, agriculture, wetlands and a few lakes in a patch type of landscape (Figure 1) characterized topographically and morphologically by a very flat sub-Cambrian peneplain. Forests, mainly conifers, are the dominating vegetation ranging from clear-felled areas to mature ca. 100 year-old stands covering an area of about 60% of the studied region (Table 1). Agriculture in this region is dominated by the cultivation of grain crops and grassland farming. Wetlands are normally undisturbed. The north-eastern corner of the area reaches the shore-line of the Gulf of Bothnia and therefore experiences some influence of sea breezes. However, easterly winds reflect the characteristics of the sea since it is a large body of water between Sweden and Finland in the southern part of the Gulf of Bothnia. South-westerly winds dominate during the summer period while the wind direction is more variable during the winter. Height differences are small, with the main part of the region confined between 30 and 70 m above sea level.

The geology is characterized by granite, sedimentary gneiss and leptite. Clayey soils and till dominate in the area. The fine-grained clay soils, together with areas of sandy and silty material, dominate in the south. Areas with till and bogs become more predominant towards the north.

The climate of this area can be characterized as warm summer continental or hemiboreal according to the Köppen classification scheme. The mean annual temperature is 5.5 °C, the mean annual precipitation is 730 mm and the mean annual runoff is between 200 and 300 mm. There is a weak increase in precipitation towards the north-east but no trends in run-off are found. The mean number of days with snow cover is ca. 100 but it varies considerably between years. The coldest month is January with a monthly mean of ca. −4 °C and the warmest month is July with a monthly mean of +17 °C. The growing season starts in mid-April and lasts *ca*. 200 days.

Figure 1. Land cover map of the study area according to the RAMS database (**left**) and CORINE database (**right**). The Norunda tower (red filled triangle) and the flight tracks (red line) for the low altitude surface flux measurements are inserted into the maps.

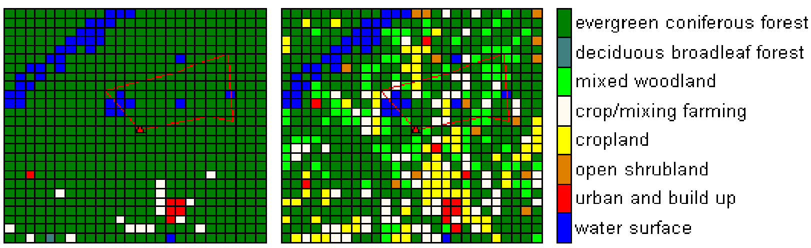

Table 1. Land-cover distribution in the studied region according to RAMS and CORINE.

Land Cover	RAMS db		CORINE db	
	Area (km^2)	Percentage of the Total Area (%)	Area (km^2)	Percentage of the Total Area (%)
Cropland	140	2.3	1,308	21.5
Deciduous forest	0	0	12	0.2
Coniferous forest	5,536	91	3,218	52.9
Mixed woodland	0	0	974	16
Wetland	0	0	97	1.6
Urban and built up areas	61	1	116	1.9
Sea and lakes	347	5.7	359	5.9
Total	6,084	100	6,084	100

2.2. Tower Site and Data

The 102 m Norunda tower is situated 60°05′10.4″N, 17°29′55.8″E in an extensively forested part of the region (Figure 1). The altitude is 45 m and the topography is flat. The vegetation surrounding the flux tower consists of *ca*. 100 year-old pine and spruce with a maximum height of 28 m with a leaf area index of 4.5. The soils are podzolised and classified as dystric regosols covered by a thin organic layer typically five cm thick. Further details about the site are given by [24].

Air temperature and humidity were measured at twelve levels of which only the one at 87.5 m was used here. Air temperatures were measured using a standard copper-constantan thermocouple, placed in ventilated radiation shields. For air humidity, air was sucked from each measurement level through a high density polyethylene tube down to an equipment shed for analysis in a gas analyzer (LI-COR, Inc., Lincoln, NE, USA). Wind velocity and direction were measured with a two-dimensional ultrasonic anemometer (Gill Basic Anemometer, Lymington, UK) at the same height as the air temperature and humidity. A detailed description of the profile measurement system is given by [26].

The eddy-correlation system for surface flux measurements consisted of a SOLENT 1012R2 sonic anemometer (Gill Instruments, Lymington, UK) and a closed path infrared gas analyzer LI-6262 (LI-COR inc., Lincoln, NE, USA). Details of the system are given by [27] and the flux calculations followed the so-called Euroflux methodology presented by [28]. Here we used data from the flux system placed at a height of 100 m because we wished to compare simulated and measured fluxes at the same height and the aircraft could not fly at lower altitude than 100 m. Since daytime gradients of temperature and humidity are extremely small above a rough surface such as a forest, it was not meaningful to compare simulated and measured state variables at lower levels than the ones chosen here.

2.3. Aircraft Data

The airborne data were acquired using aircraft during the RECAB 2001 programme in Sweden [29]. The aerial platform that was used for flux measurements is based on the certified aircraft Sky Arrow 650 ERA (Environmental Research Aircraft), a small aircraft equipped with sensors to measure three-dimensional wind and turbulence together with gas concentrations and other atmospheric parameters with high frequency. Atmospheric turbulence measurements are made with the BAT probe, which utilizes a hemispheric nine-hole pressure sphere that records static and dynamic pressures by means of four differential pressure transducers from which the velocity of air relative to the aircraft is estimated [30]. The actual wind components relative to the ground are calculated introducing corrections for three-dimensional velocity, pitch, roll and heading of the aircraft. These corrections are made using a combination of GPS and accelerometer data recording the movement of the aircraft. The probe is also equipped with a temperature sensor with a response time of 0.02 s for heat flux calculations. Mixing ratios of CO_2 and H_2O are measured at 50 Hz by a LiCor 7500 (LiCor, Lincoln, Nebraska) open path infrared gas analyzer installed downstream of the BAT probe.

Table 2. Overview of all performed vertical profile flights. z_{max} is maximum flight altitude.

Flight No.	Date	Flight Time (UTC)	z_{max} (m)
1	15.08.2001	12:17–14:00	900
2	16.08.2001	06:24–08:09	1,200
3	16.08.2001	14:12–15:52	900
4	17.08.2001	06:11–07:55	1,300
5	17.08.2001	12:14–14:11	1,600
6	18.08.2001	06:35–08:18	900
7	18.08.2001	12:08–13:51	1,300
8	19.08.2001	06:48–08:35	1,100
9	19.08.2001	10:05–11:57	1,400
10	19.08.2001	13:37–15:21	1,400
11	19.08.2001	17:07–18:47	1,100

We used data from 11 flights which were conducted during the period 16–20 August 2001 (Table 2). Flights were organized to make low-altitude (~100 m above ground level) flux measurements over heterogeneous terrain and passing over the Norunda flux tower (Figure 1). Fluxes were estimated for distances of three km but performed as a moving average giving a value for each three km. Profile measurements through the planetary boundary layer were also performed with Sky Arrow during each regular flight at Norunda tower. These flights were made as an up/down spiral centered above the Norunda tower. Previous analysis [29] has shown a good agreement between tower and airborne data.

2.4. RAMS Application

The RAMS basic equations are compressible and non-hydrostatic. The turbulent exchange is described by a so-called level 2.5 scheme [31,32] with modification for a case of growing turbulence [33]. The RAMS 4.4 version uses the Land Ecosystem Atmosphere Feedback model version 2, LEAF-2, [34] for description of energy and water vapour surface fluxes and their interactions with the atmosphere. LEAF-2 is a representation of surface features including vegetation, soil, lakes, oceans and snow cover and their influence on each other and on atmosphere. LEAF-2 includes prognostic questions for soil moisture and temperature for multiple layers, vegetation temperature and surface water including dew and intercepted rainfall, snow cover mass and thermal energy for multiple layers, as well as temperature and water vapour mixing ratio of canopy air. Here we used a soil depth of 2.1 m divided into seventeen layers. The soil type was defined as sandy loam with initial volumetric soil moisture content ranging from 0.28 to 0.31 according to measurements within the uppermost one metre of the soil profile.

RAMS simulations were performed for ten days from 14 August 2001 00:00 UTC to 24 August 2001 00:00 UTC (note that Sweden is in UTC/GMT +1 time zone) using three nested grids (Figure 2) with horizontal grid resolutions of 36, 12 and 3 km, respectively. Thirty-five layers in the vertical direction with a vertical grid spacing ranging from 25 to 1,000 m and a vertical grid stretch ratio of 5:6 (*i.e.*, $z_k/z_{k+1} = 5/6$, $z_1 = 25$, $\max\{z_k \mid \forall k\} = 1{,}000$, where z_k is the vertical grid space) were used in the simulations. The number of grid cells in the east-west and north-south directions is 26 × 26, 17 × 17 and 26 × 26 at the 36, 12 and 3 km grid resolutions, respectively. The finest grid almost covers the whole of the studied region. The time step is one minute. Four-dimensional data assimilation at lateral boundaries was employed using input global analysis fields. The data were obtained from the European Centre for Medium-Range Weather Forecasts (ERA40, ECMWF, [35,36]) at 2.5° horizontal resolution. The time interval for re-analysis fields was six hours.

A convective parameterization scheme was activated for all grids except for the three km grid. The radiation parameterization used the Chen and Cotton scheme [37]. Bulk microphysics parameterization was activated. At the top boundary of the model is a rigid lid. The lateral boundary condition is a [38] radiative condition.

Figure 2. The model domain with its three different nested grids.

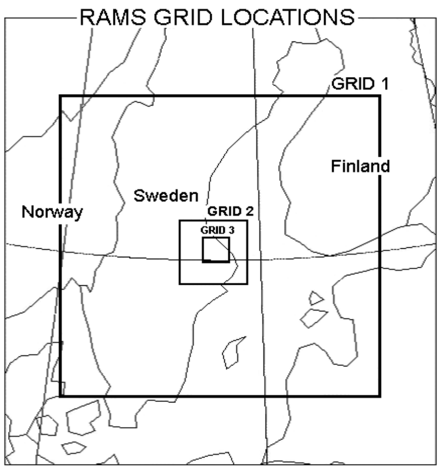

The RAMS database of vegetation cover is not very accurate for Scandinavia. The studied area has an almost homogeneous vegetation type (evergreen coniferous trees) according to the RAMS database (Table 1; Figure 1). In order to assess the importance of the land cover description we also performed simulations with a redefined vegetation database for the studied area according to the CORINE database which is much more accurate for the finer spatial scales used in this study.

The performance of the model was assessed by estimation of the root mean square error for state variables and surface fluxes as:

$$RMSE = \sqrt{\frac{\sum_{n} \left(X_{sim} - X_{obs}\right)^2}{n}} \quad (1)$$

where X_{sim} is the simulated variable, X_{obs} is the measured variable and n is the number of observations. For vertical profiles, X_{obs} is the average of aircraft values per vertical layer as defined by RAMS. This means also that n varies depending on the maximum altitude of the flights. For the comparison between tower data and RAMS, we calculated a daily RMSE based on the 48 half-hourly values obtained for each day.

The spin-up time for the simulations was two days which was enough for the atmosphere to stabilize. It usually takes longer for the soil to stabilize but since we used measured soil moisture as the initial conditions, it was not necessary to use a longer spin-up time. When comparing measured and simulated values, the simulated values were averaged to correspond to the measured ones. For tower data, this means 30 minute averages while for aircraft measurements it varies depending on the flight time.

3. Results and Discussion

All RAMS results shown in this study correspond to the RAMS simulations with three km as the highest resolution and time in UTC with 30 min output frequency.

3.1. Vertical Profiles and Boundary Layer Height

We selected a sequence of vertical flights over a period of three days, 17–19 August, that took place during and after a change from a wetter to a dryer air mass. The profile flights were carried out in the morning and around noon of all three days except on the 19th when the second flight took place at approximately 10:00 UCT. Here we compare measured data with simulated data when using the CORINE database in RAMS. The simulated profiles were averaged over the same time period as that when the flights took place. The wind speed profile was simulated very well on the morning of the 17th and also quite well for the noon flight (Figure 3). The air temperature gradient near the surface was also described well by the model although the absolute values were slightly underestimated. Relative humidity was not estimated so accurately with a noticeable overestimation by the model. It would appear that the dryer air mass entered the flight area over the Norunda tower sometime between the morning and the noon flights since the relative humidity dropped by 20–25 percentage units near the surface while the air temperature was about the same according to aircraft measurements. In contrast, the modelled relative humidity also remained high around noon (Figure 3, lower plates).

Next day, the 18th the measured and modelled temperature and humidity showed much better agreement while wind speed was overestimated in the morning (Figure 4). In the morning, the shape of the profiles also showed good agreement with gradient, shifting sign at almost the same levels. The measured and simulated profiles also showed fairly good agreement on the 19th except for wind speed in the morning where the model underestimated the speed at all levels (Figure 5). This seemed to be a matter of timing because at noon, the measured and simulated wind speed agreed very well.

Figure 3. Measured and simulated vertical profiles of the atmosphere; morning profile No. 4 (upper plates) and noon profile No. 5 (lower plates). See Table 2 for details.

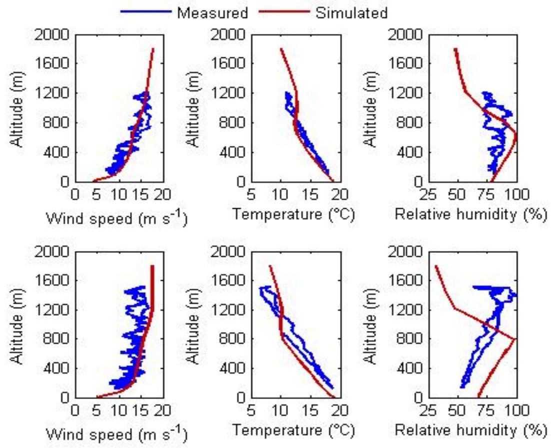

Figure 4. Measured and simulated vertical profiles of the atmosphere; morning profile No. 6 (upper plates) and noon profile No. 7 (lower plates). See Table 2 for details.

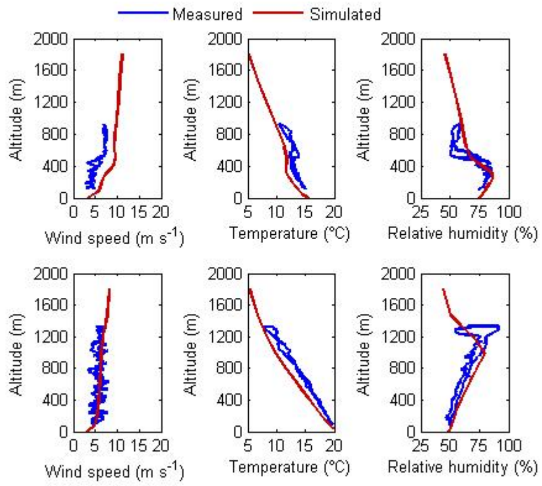

Figure 5. Measured and simulated vertical profiles of the atmosphere; morning profile No. 8 (upper plates) and noon profile No. 9 (lower plates). See Table 2 for details.

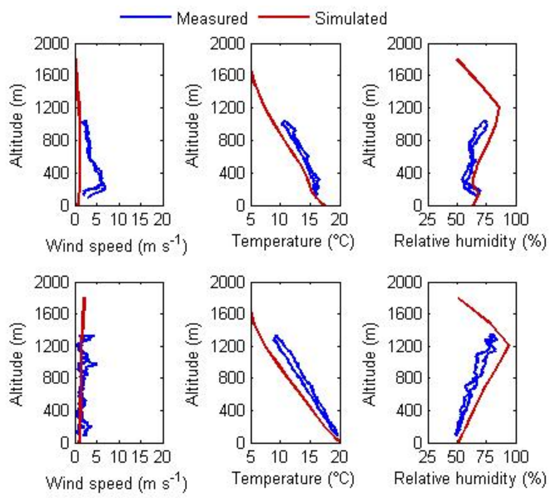

The RMSE (Equation (1)) was estimated for each one of the vertical profile flights (Table 3). The RMSE for wind speed varied between 0.95 and 3.27 m·s^{-1}, between 0.64 and 2.78 °C for air temperature and between 4.59 and 27.60% for relative humidity, respectively. The average RMSE for all profiles taken together were 1.71 m·s^{-1}, 1.56 °C and 14.16%, respectively for wind speed, air temperature and relative humidity. It is difficult to compare our RMSEs with other studies since it depends very much on the conditions under which the measurements were taken, *i.e.*, surface type, spatial and temporal scales *etc.* Chandrasekar *et al.* [20] also compared simulated and measured vertical profiles and obtained RMSE for u-wind component of 2.76–4.26 m·s^{-1}, for v-wind component 3.44–4.26 m·s^{-1}, for air temperature 1.25–2.20 °C and 41–55% for relative humidity, respectively. RMSE for wind speed and temperature are quite similar to our results but our RMSE for humidity is much smaller. Their study was performed over the city of Philadelphia so the surface conditions were much different both in terms of structure and energy partitioning.

Table 3. Root mean square error (RMSE) per flight estimated from measured and modelled vertical profiles using CORINE land cover data. Symbols are; u = wind speed, T = air temperature and RH = Relative humidity. Flight information is given in Table 2.

Flight No.	u (m·s^{-1})	T (°C)	RH (%)
1	1.20	1.26	15.33
2	1.34	1.22	16.16
3	1.55	2.19	21.54
4	1.42	1.00	11.72
5	2.67	1.78	27.53
6	2.91	1.43	7.44
7	1.09	1.62	8.25
8	2.98	1.52	9.03
9	0.95	2.08	11.53
10	1.72	2.46	23.04
11	1.23	2.31	10.23
Average	1.73	1.72	14.71

The general impression from these simulations is that the lower part of the surface layer is simulated fairly well both in shape and magnitude for wind speed, air temperature and humidity. A perfect agreement can never be expected since the observed and simulated data represent different scales. Occasionally the absolute values of the wind speed differed substantially but the shape of the profile was still well simulated. On one occasion there was a large deviation between observed and simulated air humidity which was probably caused by bad timing of the passage of a new air mass by the model. Castelli [39] used the RAMS model to simulate the meteorology over a region in the Rhine valley in Germany and they also found good agreement between observations by radio soundings and the simulated values. They found slightly worse agreement in behaviour for air humidity as compared to wind speed and air temperature. However, their vertical resolution close to the surface was not as high as in our case. Tolk [40] used the RAMS model to simulate meteorology and surface fluxes for the Cabauw region in the Netherlands and they found substantial deviations between measured and simulated vertical temperature profiles when using the standard LEAF-3 surface scheme settings. After adjustment of the model to obtain a higher Bowen ratio the agreement was much improved. We did not observe this problem using the older LEAF-2 surface scheme here but the difference between their case and ours might be found in the type of land cover characterizing the two regions; ours dominated by forest and theirs by agricultural land.

The two different methods of determining the boundary layer height based on simulations gave quite different results (Figure 6(a)). The first method is based on turbulent kinetic energy (TKE):

$$h_{PBL} = z\left(1 - \frac{z_T}{Z}\right), \tag{2}$$

where z is the minimum of height where TKE is less than the specified threshold (0.001 $m^2 \cdot s^{-2}$), z_T is the topography height and Z is the height of model top. The second method used the potential temperature and the absolute air humidity ($g \cdot kg^{-1}$) and visual analysis of their profiles. The height where profiles make a jump/knee is defined as PBL height. The method based on TKE (Equation (2)) generally indicated higher PBL than the ones determined from profiles. The PBL determined from aircraft measured profiles were in better agreement with the corresponding ones estimated from simulations. On some occasions it was not possible to estimate PBL height from aircraft because of too low flight altitudes.

Figure 6. (**a**) The simulated (with CORINE land-cover data) boundary layer (PBL) height defined via turbulent kinetic energy (TKE) (red line), the simulated (with CORINE land-cover data) PBL defined via relative temperature and absolute air humidity ($g \cdot kg^{-1}$) (red filled circle), the defined PBL via relative temperature and absolute air humidity from the aircraft measured values for up/down spiral (triangle up/down), maximum height of flight (green filled circle). (**b**) The difference in boundary layer height estimation between CORINE and RAMS land-cover data (RAMS values—CORINE values).

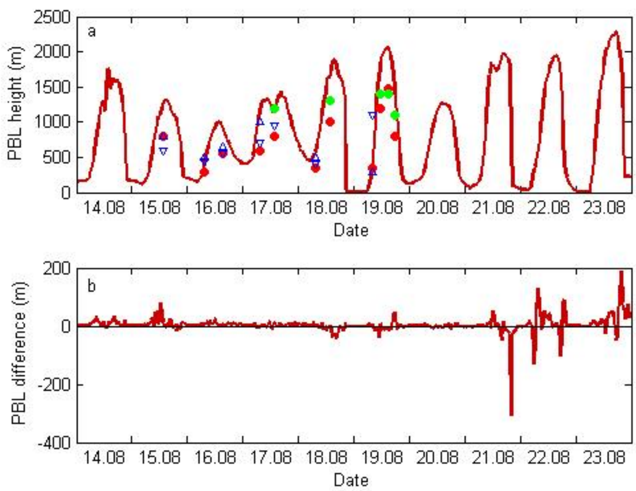

We also tested the importance of land cover representation for the PBL height and for most of the days the differences were small but occasionally larger differences occurred (Figure 6(b)). The maximum simulated PBL height during the ten day period was 2,200 m for the TKE method and 1,500 m for the profile method (Figure 6(a)). The high PBL is a well known feature of boreal ecosystems caused by prominent convection. Shaskov [41] measured vertical profiles over some Canadian boreal forest and found PBL heights up to 2,550 m during a period in July 2002. Gryning and Batchvarova [42] estimated PBL height over the same region as we did and found values up to about 2,000 m over three summer days in 1994.

3.2. Surface Fluxes and Meteorology

Here we compare the 87.5 m height modelling level with the measurements of sensible and latent heat fluxes in tower and by aircraft, and air temperature, air humidity and wind speed with the measurements in the Norunda tower at the same height. We choose to compare the simulated and measured values at the highest levels in the tower because; (a) the fluxes measured at this height have a larger footprint than the fluxes measured just above the forest and this footprint is closer in size to the aircraft as well as the simulated footprint and (b) the state variables at this level are less influenced by the 28 m high forest whose profiles are not simulated by RAMS. The model represents the temporal variation of the wind speed, the air temperature and the air humidity (mixing ratio) quite well (Figure 7). During the first few days of the period the simulated maximum temperature lags slightly behind the measured one but later in the period the two maxima synchronise well. The largest difference between modelled and measured temperature occurred on the 20th of August with maximum differences of the order of 5 °C (Figure 7). This was a special day with heavy overcast conditions and with rain showers during the day. This was not captured by the model which simulated an almost cloud-free day. The effect of using different land cover data, RAMS and CORINE respectively, on the state variables was practically negligible (Figure 7). This is reasonable because around the Norunda tower, the vegetation type is similar in both land-cover databases.

Figure 7. Measured and simulated wind speed (upper), air temperature (middle) and air humidity mixing ratio (lower) for the ten-day period in August 2001.

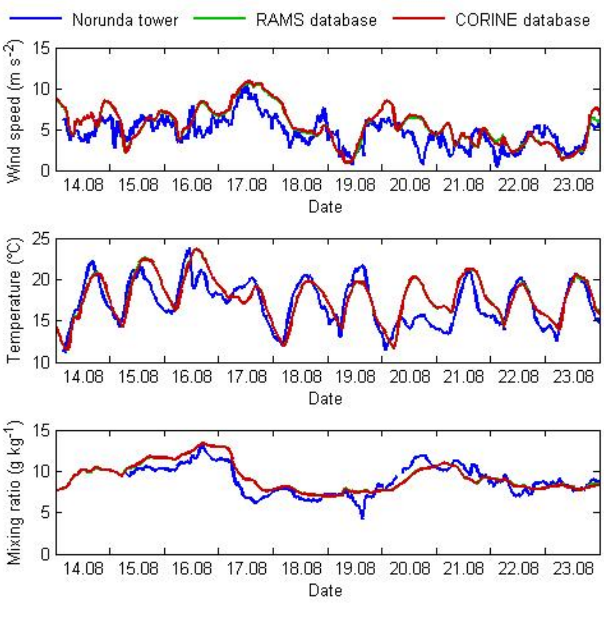

The measured sensible and latent heat fluxes in the tower show relatively large short term variability which is characteristic for turbulent fluxes measured at a point (Figure 8). The modelled fluxes are generally much smoother with a few exceptions such as the 14th and the 21st of August. The modelled sensible heat fluxes show an increasing trend of higher and higher maximum values, a trend which is not seen in the tower fluxes. The opposite trend is seen for latent heat fluxes where the modelled ones decrease over time (Figure 8). The fluxes measured by aircraft match the fluxes measured at the tower slightly better than the modelled ones. The largest deviation between measured and modelled fluxes occurred on the 20th of August when the tower fluxes were close to zero during the whole day while the modelled fluxes showed similar values as compared to adjacent days. The 20th of August was heavily overcast all day which was not reflected by the model. It is interesting to note that the correspondence between measured and modelled fluxes is quite close at night.

Figure 8. Measured and simulated sensible heat flux (**upper**) and latent heat flux (**lower**) for the ten-day period in August 2001. The thin lines in the figure represent simulation with +10% respectively −10% lower initial values of soil moisture.

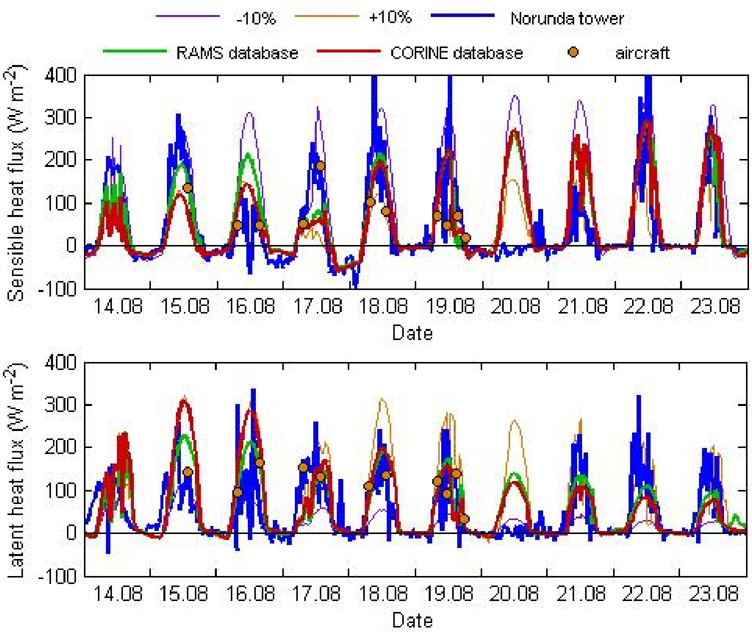

The increasing trend in sensible heat fluxes and a corresponding decreasing trend in latent heat fluxes are probably caused by too much sensitivity to soil moisture which is clearly demonstrated by the simulations with +10% respectively −10% difference in initial soil moisture. The ten-day period simulated here occurred during a period of fine weather with drying soils and we could conclude that the model was sensitive to initial soil moisture. The model run was initiated with the measured soil moisture profile but, with another initialization, the trend would have disappeared.

Another possible explanation of the deviation between measured and simulated fluxes is differences in net radiation and soil heat fluxes. However, we compared measured and simulated net radiation and agreement was quite good in general except for the rainy day of 20th August so this explanation is less likely.

The temporal development of states and fluxes are in general well described by the model. Exceptions occur when the model failed to simulate the cloudiness correctly. Again, this can probably be explained largely by the mismatch in scales between observations and simulated values. Our results are very similar to those obtained by [40] where they compared the lowest modelling level with data on meteorology in the 200 m high Cabauw tower and surface fluxes from different type of ecosystems. Interestingly, their simulations of sensible heat fluxes for the forested site agreed almost perfectly (for the two days shown) with observations for both of the two different Bowen ratio settings.

Table 4. RMSE per day estimated from modelled and measured half-hourly tower fluxes and meteorology using CORINE land cover data. Symbols are: u = wind speed, T = air temperature, ω = air humidity mixing ratio, H = sensible heat flux and LE = latent heat flux.

Date	u (m·s^{-1})	T (°C)	ω (g·kg^{-1})	H(W·m^{-2})	LE (W·m^{-2})
14.08.2001	1.82	1.33	no data	68.40	78.51
15.08.2001	1.62	2.17	1.11	67.65	102.61
16.08.2001	2.07	2.23	1.18	61.35	109.49
17.08.2001	2.15	1.31	1.62	67.59	60.54
18.08.2001	1.77	1.34	0.52	98.30	50.26
19.08.2001	1.20	1.25	1.06	61.74	51.46
20.08.2001	2.57	3.26	1.20	144.42	62.15
21.08.2001	1.69	2.40	0.93	87.46	46.45
22.08.2001	1.22	1.14	0.69	64.39	67.17
23.08.2001	1.16	0.89	0.39	50.61	45.40
Average	1.73	1.73	0.97	77.19	67.40

The RMSE for air temperature ranged between 1.16 and 2.57 °C and between 0.89 and 3.26 m·s^{-1} for wind speed for the ten days presented in Table 4. These RMSE values are quite similar to the results found by Carvalho *et al.* [43] who applied the RAMS model over a 300 × 300 km^2 area of complex terrain in the south western part of Germany, eastern part of France and the northern part of Switzerland in a tracer experiment. They had a number of ground stations with measured air temperature and wind speed to compare model results with and they obtained daily RMSE in the range 1.19 and 3.25 m·s^{-1} for wind speed and 1.94 to 5.33 °C for air temperature, respectively, for seven of their selected stations. The station which showed the lowest RMSE was close to our results. The average RMSE for wind speed was 1.73, for air temperature 1.73 °C, for mixing ratio 0.97 g·kg^{-1}, for sensible heat flux 77.19 W·m^{-2} and for latent heat flux 67.40 W·m^{-2} (Table 4). The largest error occurred on the 20th of August when the model failed to simulate the cloudiness (and radiation) correctly. It has been noted in similar mesoscale modelling studies that the exact location of clouds and, thus, the timing of radiation sometimes deviate from observations (e.g., [44]). The relatively large RMSE for the diurnal courses of surface fluxes are partly caused by the large variation in the measured fluxes which is not represented by the model for reasons explained below. It is partly explained by the model's inability to estimate correctly the timing and location of clouds which will have a large effect on the fluxes in a particular grid cell. In addition, tower measurements are performed in a turbulent atmosphere and even if we use half-hourly time averaging, there will always be a large temporal variability of fluxes. The flux measurements are measured at a point, or rather in a small volume, in the atmosphere and in order to have more accurate areal representation, we would need to have many measurement points above the vegetation. The results are much better when comparing the average for the whole ten-day period; the measured and simulated sensible heat fluxes are 40.5 and 47.3 W·m^{-2}, respectively and the corresponding values for latent heat fluxes are 45.9 and 57.0 W·m^{-2}, respectively.

We cannot rule out the possibility that this better agreement, when averaging over a longer period of time, is an effect of cancelling errors, but considering the mismatch in spatial scale between the point measurements and the area-"averaged" modelled values, it is not unreasonable to assume that the improvement is at least partly caused by the smoothing of random errors due to the averaging procedure.

3.3. Sensitivity to Land-Cover Type and Soil Moisture

For the study region selected here the RAMS land-cover data base contains an over-representation of forest (Table 1; Figure 1). The CORINE database gives a much more realistic description of the land-cover with a substantially higher fraction of open land as compared to the RAMS database. The CORINE land cover for the flight track was quite similar in distribution as compared to the whole area of the finest grid. The comparison between area-averaged measurements by aircraft, here averaged over the whole flight track (see Figure 1) and the corresponding area-averaged simulated values for the whole area of the finest grid, show that occasionally there are large differences between measured and simulated values, as for example for flight track No. 4 where latent heat flux is underestimated by the model of the order of 150 $W \cdot m^{-2}$ for both RAMS and CORINE simulations (Figure 9(A,C)) while the sensible heat flux is in reasonable agreement (Figure 9 (B and D)). The opposite situation can also be found where latent heat flux is in good agreement, e.g., flight No. 9 (with original initial values for soil moisture) while sensible heat flux shows a large deviation (Figure 9(B,D)). We tested the sensitivity to soil moisture by changing the initial values of the soil moisture profile by ±10% and the results clearly demonstrate the considerable sensitivity to soil moisture (Figure 9). The average difference over all eight flights between measured and simulated latent heat flux was −29.8 $W \cdot m^{-2}$ and −28.9 $W \cdot m^{-2}$ for RAMS and CORINE databases respectively when using the measured soil moisture profile at Norunda for the initial values (Table 5). The corresponding values for sensible heat fluxes were 9.2 $W \cdot m^{-2}$ and 23.2 $W \cdot m^{-2}$, respectively. The model thus underestimated the latent heat fluxes and overestimated the sensible heat fluxes. However, increasing initial soil moisture by 10% considerably improved the balance between latent and sensible heat fluxes (Table 5) resulting in better agreement between measured and simulated values in terms of overall averages although the variance did not improve (Table 5). We can also note that the difference between using RAMS land cover or CORINE land cover had some but not a negligible effect on the area-averaged values (Figure 9 and Table 5). This might however be a consequence of the fact that the flight track was dominated by forests and in that case, the difference between the two data bases was not so large.

We also chose to illustrate the effect of land-cover differences by comparing the sensible and latent heat fluxes simulated at noon for the whole region for the first and the last day of the ten-day period (Figures 10 and 11). We can first of all note that the spatial variation can be quite marked on certain days while it can also be more homogeneous for other days. This variability is a reflection of variations both in meteorology and land-cover. The successive decrease in latent heat fluxes and corresponding increase in sensible heat fluxes over time can be clearly seen here. The latent heat flux at the end of the ten-day period has decreased down to a maximum of about 150 $W \cdot m^{-2}$ as compared to the maximum of about 350 $W \cdot m^{-2}$ at the beginning of the period. The difference in surface fluxes between RAMS and CORINE land-cover data is illustrated in Figure 11. There are spatial patterns that are consistent between the different days and this is most likely a direct effect of the differences in land-cover.

Averaged over the whole region, the difference in latent heat flux varied between −12 (day No. 2) and 21 W·m^{-2} (day No. 10) and between −13 (day No. 6) and 15 W·m^{-2} (day No. 1). Thus, averaging over the whole region did not diminish the differences completely.

We are aware that the more recent version 6.0 of RAMS with the LEAF-3 sub-model for surface exchanges contains the option to use satellite derived NDVI to provide more specific data on vegetation than the current version 4.4 used in this study. However, the under-lying land cover is still the same in version 6.0 as in version 4.4 which means that in our region it is a big mismatch between the actual land cover and those used in the RAMS database. We believe that our results illustrate a worst case scenario showing the effect of replacing a practically homogeneous vegetation cover (coniferous forest) with a realistic mosaic type of landscape with mixed forest, cropland, open land etc and that this provides information on the importance of proper land cover representation.

Figure 9. Area-averaged surface fluxes from aircraft (filled circle) and simulations using RAMS land cover (**A**,**B**) CORINE land cover respectively (**C**,**D**). The flight numbers on the x-axis are the same as in Table 2. Simulated values are based on: measured initial soil moisture at Norunda tower (square), +10% increase of soil moisture (triangle up) and −10% decrease of soil moisture (triangle down). The area averaged simulated values are the mean of all grid cells in the finest grid (grid No. 3 in Figure 2).

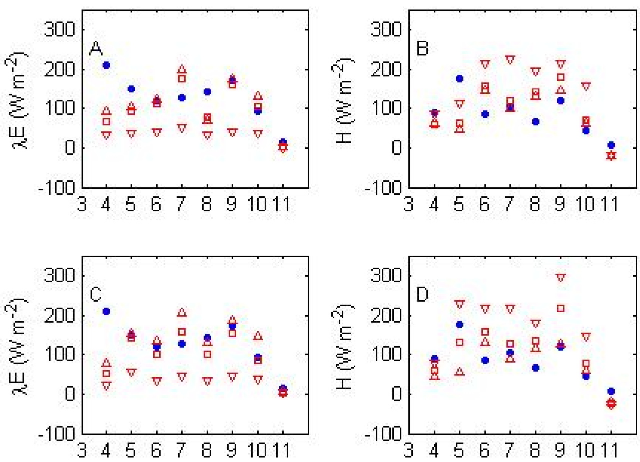

Table 5. Mean and standard deviation of the differences between area-averaged aircraft measured values and simulated ones from Figure 9.

		Latent Heat Flux (W·m^{-2})	Sensible Heat Flux (W·m^{-2})
	soil profile	−29.80 ± 57.45	9.23 ± 64.37
RAMS	−10%	−94.79 ± 49.89	60.35 ± 79.12
	+10%	−15.97 ± 60.64	−2.25 ± 60.98
	soil profile	−28.92 ± 56.50	23.21 ± 53.56
CORINE	−10%	−95.36 ± 51.46	79.64 ± 72.62
	+10%	1.04 ± 62.34	−11.56 ± 55.27

Figure 10. The simulated sensible (**left**) and latent heat fluxes (**right**) for the first and last day of the 10-day period (numbered 1 and 10). Values are for noon each day.

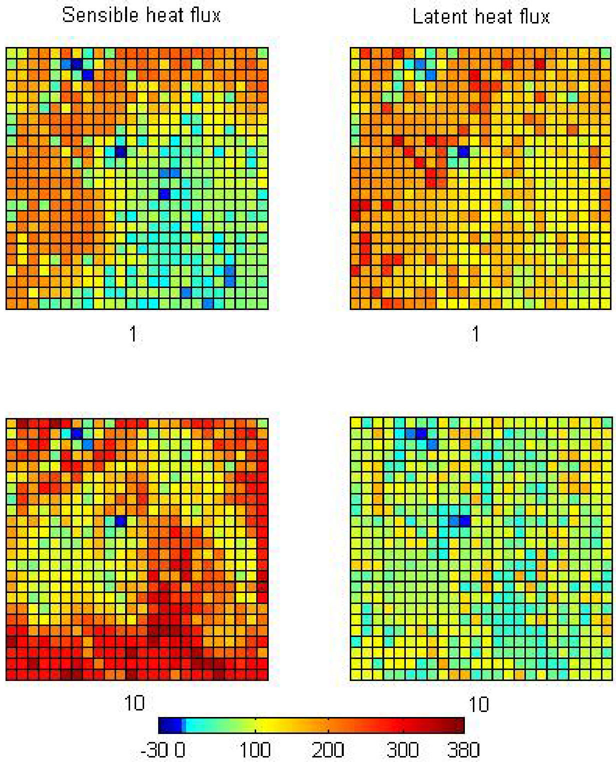

Figure 11. The difference in sensible (**left**) and latent heat fluxes (**right**) when using RAMS and CORINE land-cover data (CORINE values—RAMS values).

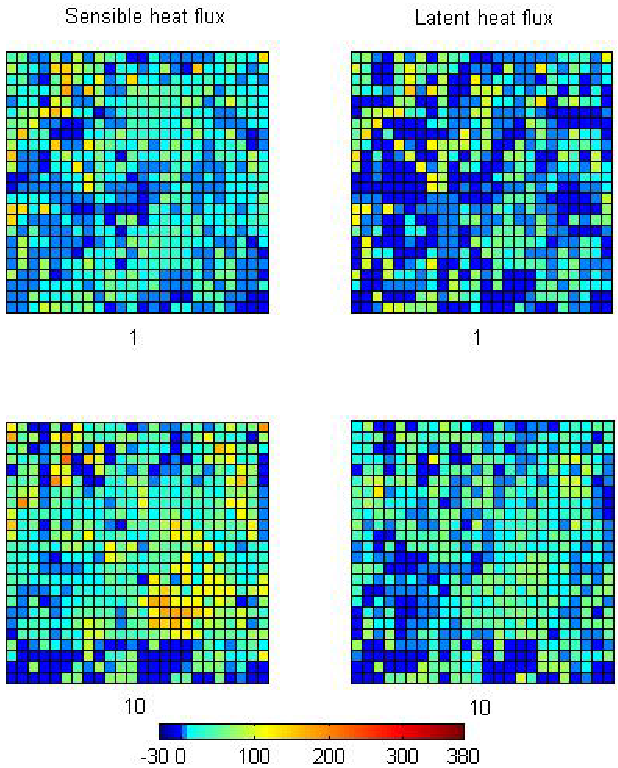

4. Conclusions

In this study we examined how well a mesoscale model, RAMS, could simulate meteorology and fluxes above a boreal region in Sweden. We made a detailed comparison against measured data in a high tower located within a boreal forest area and against low altitude flight flux measurements and vertical boundary-layer profiles with an aircraft. We found that the RAMS model can provide a reasonably accurate representation of meteorology in time as well as vertically in the atmosphere but at the same time that surface fluxes are less well simulated with relatively large biases in magnitude as well as in the partitioning between latent and sensible heat fluxes. Some of these biases were caused by differences between simulated and observed radiation which in turn was linked to differences in cloudiness. However, the most noticeable feature was the model's oversensitivity to soil moisture which had a large effect on the partitioning between sensible and latent heat fluxes. The sensitivity to soil moisture was not found in the observations. We thus conclude that further studies of the models sensitivity to soil moisture is deemed necessary before the model can be used with confidence in boreal environments. The model is also sensitive to land cover type which is important for the spatial distribution of surface fluxes as well as for the area averaged fluxes. This result was not unexpected and it demonstrates the importance of proper land cover representation in the model.

Acknowledgments

The Nordic Council of Ministers, NOS-N, the Swedish Research Council and the Knut and Alice Wallenberg foundation are all acknowledged for their financial support. The study was performed within the framework of the Nordic NCoE programme on climate change, the NECC (Nordic Centre for Studies of Ecosystem Carbon Exchange and Climate Interactions) and within the strong research environment, LUCCI at Lund University.

We thank Craig J. Tremback kindly for an important contribution at the ATMET forum which was created to support RAMS users. This forum is very useful especially for beginners.

Conflict of Interest

The authors declare no conflict of interest.

References

1. Claussen, M.; Cox, P.M.; Zeng, X.; Viterbo, P.; Beljaars, A.C.M.; Betts, R.A.; Bolle, H.-J.; Chase, T.; Koster, R. The Global Climate. In *Vegetation, Water, Humans and the Climate: A New Perspective on an Interactive System*; Springer-Verlag: Heidelberg, Germany, 2004; pp. 33–57.
2. Rummukainen, M.; Bergstrom, S.; Persson, G.; Rodhe, J.; Tjernstrom, M. The Swedish Regional Climate Modelling Programme, SWECLIM: A review. *Ambio* **2004**, *33*, 176–182.
3. Brovkin, V.; Claussen, M.; Driesschaert, E.; Fichefet, T.; Kicklighter, D.; Loutre, M.F.; Matthews, H.D.; Ramankutty, N.; Schaeffer, M.; Sokolov, A. Biogeophysical effects of historical land cover changes simulated by six earth system models of intermediate complexity. *Climate Dyn.* **2006**, *26*, 587–600.

4. Bathiany, S.; Claussen, M.; Brovkin, V.; Raddatz, T.; Gayler, V. Combined biogeophysical and biogeochemical effects of large-scale forest cover changes in the MPI earth system model. *Biogeosciences* **2010**, *7*, 1383–1399.
5. Eastman, J.L.; Coughenour, M.B.; Pielke, R.A. The regional effects of CO_2 and landscape change using a coupled plant and meteorological model. *Glob. Change Biol.* **2001**, *7*, 797–815.
6. Pielke, R.A.; Cotton, W.R.; Walko, R.L.; Tremback, C.J.; Lyons, W.A.; Grasso, L.D.; Nicholls, M.E.; Moran, M.D.; Wesley, D.A.; Lee, T.J.; *et al*. A comprehensive meteorological modeling system—RAMS. *Meteor. Atmos. Phys.* **1992**, *49*, 69–91.
7. Cox, R.; Bauer, B.L.; Smith, T. A mesoscale model intercomparison. *Bull. Amer. Meteorol. Soc.* **1998**, *79*, 265–283.
8. ENVIRON International Corporation; Mission Research Corporation. *MM5/RAMS Fine Grid Meteorological Modelling for September 8–11, 1993 Ozone Episode*; TNRCC Report; Texas Natural Resources Conservation Commission: Austin, TX, USA, 2001. Available online: www.tceq.texas.gov/assets/public/implementation/air/am/contracts/reports/mm/MM5-RAMS-FineGridMetModeling.pdf (accessed on 27 October 2012).
9. Taylor, C.M.; Harding, R.J.; Pielke, R.A.; Vidale, P.L.; Walko, R.L.; Pomeroy, J.W. Snow breezes in the boreal forest. *J. Geophys. Res.* **1998**, *103*, 23087–23101.
10. Melas, D.; Persson, T.; de Bruin, H.; Gryning, S.-E.; Batchvarova, E.; Zerefos, C. Numerical model simulations of boundary-layer dynamics during winter conditions. *Theor. Appl. Climatol.* **2001**, *70*, 105–116.
11. Savijärvi, H.; Amnell, T. High resolution flight observations and numerical simulations: Horizontal variability in the wintertime boreal boundary layer. *Theor. Appl. Climatol.* **2001**, *70*, 245–252.
12. Bergström, H.; Juuso, N. A study of valley winds using the MIUU meso-scale model. *Wind Energy* **2006**, *9*, 109–129.
13. Chapin, F.S., III; McGuire, A.D.; Randerson, J.; Pielke, R.A.; Baldocchi, D.; Hobbie, S.E.; Roulet, N.; Eugster, W.; Kasischke, E.; Rastetter, E.B.; *et al*. Arctic and boreal ecosystems of western North America as components of the climate system. *Glob. Change Biol.* **2000**, *6*, 211–223.
14. Pielke, R.A.; Uliasz, M. Use of meteorological models as input to regional and mesoscale air quality models—Limitations and strengths—Radiative balance and visual air quality. *Atmos. Environ.* **1998**, *32*, 1455–1466.
15. Buckley, R.L.; Weber, A.H.; Weber, J.H. Statistical Comparison of Forecast Meteorology with Observations Using the Regional Atmospheric Modeling System. Available online: http://sti.srs.gov/fulltext/ms2001678/ms2001678.html (accessed on 23 September 2011).
16. Doty, K. *Ad Hoc* Meteorological Modeling Group: August 2001 Meeting Summary. Available online: www.epa.gov/scram001/adhoc/sum2001.pdf (accessed on 12 May 2008).
17. Sistla, G.; Hao, W.; Ku, J.Y.; Kallos, G.; Zhang, K.S.; Mao, H.T.; Rao, S.T. An operational evaluation of two regional-scale ozone air quality modeling systems over the eastern United State. *Bull. Amer. Meteorol. Soc.* **2001**, *82*, 945–964.
18. Zhang, K.; Mao, H.; Civerolo, K.; Berman, S.; Ku, J.Y.; Rao, S.T.; Doddridge, B.; Philbrick, C.R.; Clark, R. Numerical investigation of boundary-layer evolution and nocturnal low-level jets: Local *versus* non-local PBL schemes. *Environ. Fluid Mech.* **2001**, *1*, 171–208.

19. Fast, J.D. The Relative Role of Local and Regional-Scale Processed on Ozone in Philadelphia. In *Proceeding of the Fourth Conference on Atmospheric Chemistry: Urban, Regional, and Global-Scale Impacts of Air Pollutants*; American Meteorological Society: Orlando, FL, USA, 2002; pp. 121–124.
20. Chandrasekar, A.; Philbrick, R.C.; Doddridge, B.; Clark, R.; Georgopoulos, P. A comparison study of RAMS simulations with aircraft, wind profiler, lidar, tethered balloon and RASS data over Philadelphia during a 1999 summer episode. *Atmos. Environ.* **2003**, *37,* 4973–4984.
21. Atmospheric, Meteorological and Environmental Technologies. Available online: http://atmet.com/ (accessed on 27 October 2012).
22. Halldin, S.; Gottschalk, L.; van de Griend, A.A.; Gryning, S.-E.; Heikinheimo, M.; Hogstrom, U.; Jochum, A.; Lundin, L.-C. *Science Plan for NOPEX*; NOPEX Technical Report No. 12; Uppsala University, NOPEX Central Office: Uppsala, Sweden, 1995; p. 38.
23. Halldin, S.; Gottschalk, L.; van de Griend, A.A.; Gryning, S.-E.; Heikinheimo, M.; Hogstrom, U.; Jochum, A.; Lundin, L.-C. NOPEX-A northern hemisphere climate processes land surface experiment. *J. Hydrol.* **1998**, *212–213*, 172–187.
24. Lundin, L.-C.; Halldin, S.; Lindroth, A.; Cienciala, E.; Grelle, A.; Hjelm, P.; Kellner, E.; Lundberg, A.; Mölder, M.; Moren, A.-S.; *et al*. Continuous long-term measurements of soil-plant-atmosphere variables at a forest site. *Agr. Forest Meteorol.* **1999**, *98–99*, 53–73.
25. Xu, C.-Y.; Seibert, J.; Halldin, S. Regional water balance modelling in the NOPEX area: Development and application of monthly water balance models. *J. Hydrol.* **1996**, *180*, 211–236.
26. Mölder, M.; Lindroth, A.; Halldin, S. Water vapor, CO_2, and temperature profiles in and above a forest—Accuracy assessment of an unattended measurement system. *J. Atmos. Ocean. Technol.* **2000**, *17*, 417–425.
27. Grelle, A.; Lindroth, A. Eddy-correlation system for long-term monitoring of fluxes of heat, water vapour and CO_2. *Global Change Biol.* **1996**, *2*, 297–307.
28. Aubinet, M.; Grelle, A.; Ibrom, A.; Rannik, Ü.; Moncrieff, J.; Foken, T.; Kowalski, A.S.; Martin, P.H.; Berbigier, P.; Bernhofer, C.; *et al.* Estimates of the annual net carbon and water exchange of forests: The EUROFLUX methodology. *Adv. Ecol. Res*. **2000**, *30*, 113–175.
29. Gioli, B.; Miglietta, F.; de Martino, B.; Hutjes, R.; Dolman, H.; Lindroth, A.; Schumacher, M.; Sanz, M.; Manca, G.; Peressotti, A.; *et al*. Comparison between tower and aircraft-based eddy covariance fluxes in five European regions. *Agr. Forest Meteorol.* **2004**, *127*, 1–16.
30. Crawford, T.L.; Dobosy, R.J. A sensitive fast-response probe to measure turbulence and heat flux from any airplane. *Bound. Lay. Meteorol.* **1992**, *59*, 257–278.
31. Mellor, G.L.; Yamada, T. A hierarchy of turbulence closure models for planetary boundary layers. *J. Atmos. Sci.* **1974**, *31*, 1791–1806.
32. Mellor, G.L.; Yamada, T. Development of a turbulence closure model for geophysical fluid problems. *Rev. Geophys. Space Phys.* **1982**, *20*, 851–875.
33. Helfand, H.M.; Labraga, J.C. Design of a nonsingular level 2.5 second-order closure model for the prediction of atmospheric turbulence. *J. Atmos. Sci*. **1988**, *45*, 113–132.
34. Walko, R.L.; Band, L.E.; Baron, J.; Kittel, T.G.F.; Lammers, R.; Lee, T.J.; Ojima, D.S.; Pielke, R.A.; Taylor, C.; Tague, C.; Tremback, C.J.; Vidale, P.L. Coupled atmosphere-biophysics-hydrology models for environmental modeling. *J. Appl. Meteor*. **2000**, *39*, 931–944.

35. European Centre for Medium-Range Weather Forecasts. Available online: http://www.ecmwf.int/ (accessed on 27 October 2012).
36. Uppala, S.M.; Kellberg, P.W.; Simmons, A.J.; Andrae, U.; da Costa Bechtold, V.; Fiorino, M.; Gibson, J.K.; Haseler, J.; Hernandez, A.; Kelly, G.A.; *et al.* The ERA-40 re-analysis. *Q. J. R. Meteorol. Soc*. **2005**, *131*, 2961–3012.
37. Chen, C.; Cotton, W.R. A one-dimensional simulation of the stratocumulus-capped mixed layer. *Bound. Lay. Meteorol.* **1983**, *25*, 289–321.
38. Klemp, J.B.; Wilhelmson, R.B. The simulation of three-dimensional convective storm dynamics. *J. Atmos. Sci.* **1978**, *35*, 1070–1096.
39. Castelli, S.T.; Morelli, S.; Anfossi, D.; Carvalho, J.; Zauli Sajani, S. Intercomparison of two models, ETA and RAMS, with TRACT field campaign data. *Environ. Fluid Dynam.* **2004**, *4*, 157–196.
40. Tolk, L.F.; Peters, W.; Meesters, A.G.C.A.; Groenendijk, M.; Vermeulen, A.T.; Steeneveld, G.J.; Dolman, A.J. Modelling regional scale surface fluxes, meteorology and CO_2 mixing ratios for the Cabauw tower in the Netherlands. *Biogeosciences* **2009**, *6*, 2265–2280.
41. Shashkov, A.; Higuchi, K.; Chan, D. Aircraft vertical profiling of variation of CO_2 over a Canadian boreal forest site: A role of advection in the changes in the atmospheric boundary layer CO_2 content. *Tellus* **2007**, *59B*, 234–243.
42. Gryning, S.-E.; Batchvarova, E. Regional heat flux over the NOPEX area estimated from the evolution of the mixed-layer. *Agr. Forest Meteorol.* **1999**, doi:org/10.1016/S0168-1923(99)00095-7.
43. Carvalho, J.; Anfossi, D.; Trini Castelli, S.; Degrazia, G. Application of a model system for the study of transport and diffusion in complex terrain to the TRACT experiment. *Atmos. Environ.* **2002**, *36*, 1147–1161.
44. Denning, A.S.; Nicholls, M.; Prihodko, L.; Baker, I.; Vidale, P.L.; Davis, K.; Bakwin, P. Simulated variations in atmospheric CO_2 over a Wisconsin forest using a coupled ecosystem-atmosphere model. *Glob. Change Biol.* **2003**, *9*, 1241–1250.

© 2012 by the authors; licensee MDPI, Basel, Switzerland. This article is an open access article distributed under the terms and conditions of the Creative Commons Attribution license (http://creativecommons.org/licenses/by/3.0/).